binding α subunits with high affinity, preventing binding of the DNA target sequence. It is also possible that the SMMHC protein contributes a domain that results in inappropriate transcriptional regulation by the α/β complex. Finally, the CBFβ-SMMHC dimers may acquire some new activity in transcriptional regulation.

The elucidation of these two genes as the fusion partners in an inversion leading to a common form of adult leukemia should also allow the development of a mouse model and a sensitive RT-PCR test for specific diagnosis and assessment of residual disease after treatment. Complete elucidation of the mechanisms by which CBFβ-SMMHC transforms a particular hematopoietic lineage may eventually lead to new and more effective therapies for this relatively common form of adult leukemia.

REFERENCES AND NOTES

1. P. Leder *et al.*, *Science* **222**, 765 (1983); L. R. Finger, R. C. Harvey, R. C. A. Moore, L. C. Showe, C. M. Croce, *ibid.* **234**, 982 (1986).
2. J. Borrow, A. D. Goddard, D. Sheer, E. Solomon, *ibid.* **249**, 1577 (1990); H. de Thé, C. Chomienne, M. Lanotte, L. Degos, A. Dejean, *Nature* **347**, 558 (1990).
3. D. C. Arthur and C. D. Bloomfield, *Blood* **61**, 994 (1983); M. M. Le Beau *et al.*, *N. Engl. J. Med.* **309**, 630 (1983); F. Mitelman and S. Heim, *Genes Chromosomes Cancer* **5**, 57 (1992); S. Heim and F. Mitelman, *Cancer Suppl.* **70**, 1701 (1992).
4. Fourth International Workshop on Chromosomes in Leukemia, 1982, *Cancer Genet. Cytogenet.* **11**, 275 (1984).
5. J. M. Bennett *et al.*, *Ann. Intern. Med.* **103**, 620 (1985).
6. P. Liu *et al.*, *Blood*, in press.
7. We conducted Alu-PCR [P. Liu *et al.*, *Cancer Genet. Cytogenet.* **65**, 93 (1993)] with DNA from YAC clones yB80B9, y854E2, y757D7, and yC8E12 and the 35B11 cosmid contig and separated the PCR products by agarose gel electrophoresis. The PCR products in common in yB80B9, y854E2, and y757D7 [these three YAC clones contain the p arm breakpoint (*6*)] but not present in yC8E12 and the cosmid contig [they do not contain the p arm breakpoint (*6*)] were excised from the gel. The DNA was purified from the agarose and used as a probe to screen the chromosome 16 cosmid library. Positive clones were picked and further studied.
8. K. Yanagisawa, T. Horiuchi, S. Fujita, *Blood* **78**, 451 (1991).
9. P. Liu, S. A. Tarlé, A. Hajra, F. S. Collins, unpublished data.
10. D. F. Callen *et al.*, *Genomics* **13**, 1178 (1992).
11. Z. Deng *et al.*, *ibid.*, in press.
12. D. F. Callen *et al.*, *Am. J. Hum. Genet.* **51**, A57 (1992); J. W. Wessels *et al.*, *Blood* **77**, 1555 (1991); J. G. Dauwerse *et al.*, *ibid.* **79**, 1299 (1992).
13. The cosmid library was constructed as follows: The genomic DNA from the leukemia cells of an inv(16) patient was partially digested with Mbo I to an average size of 40 kb, and the ends were filled in with deoxyguanosine triphosphate and deoxyadenosine triphosphate. The sCOS vector [G. A. Evans, K. Lewis, B. E. Rothenberg, *Gene* **79**, 9 (1989)] was modified by inserting an Xho I linker at the Bam HI site (performed by D. A. Marchuk). The vector was digested with Xho I and Xba I, and the ends were filled in with deoxythymidine triphosphate and deoxycytidine triphosphate. The digested genomic DNA and the vector were then ligated and packaged by means of a commercial packaging kit (Gigapack Gold, Stratagene). The phage particles containing cosmid DNA were transducted into *Escherichia coli* A490 cells.
14. A. Swaroop and J. Xu, *Cytogenet. Cell Genet.*, in press.
15. During the preparation of this manuscript, Matsuoka *et al.* reported the cloning of a human SMMHC gene, *MYH11* [R. Matsuoka *et al.*, *Am. J. Med. Genet.* **46**, 61 (1993)]. The sequence of this gene is identical to that of L11a for 1.8 kb except for a few nucleotide differences (<0.3%) which are most likely due to sequencing errors [L11a contains a sequence corresponding to nucleotides (nt) 1579 through 3364 of that reported by Matsuoka *et al.*]. By correlating hybridization intensity and gene dosage on Southern blot and FISH, Matsuoka *et al.* regionally assigned *MYH11* to 16q12. From the results described in this report and more extended studies described elsewhere, which also indicate that there is only a single locus for *MYH11* (*11*), we conclude that the location of *MYH11* on chromosome 16 is actually in the region 16p13.12–p13.13, spanning the p arm breakpoint of inv(16).
16. C. Peterson and R. Legerski, *Gene* **107**, 279 (1991).
17. S. Wang *et al.*, *Mol. Cell. Biol.* **13**, 3324 (1993).
18. The GenBank accession number for partial human *CBFB* cDNA sequence is L20298. The sequence of nucleotides 1 through 57 was derived from an RT-PCR product with RNA of inv(16)-positive leukemic cells using a primer with the sequence of the first six codons of the mouse CBFβ gene and primer M1 (*20*). The rest of the sequence was from the cDNA clone RL9a.
19. P. Marlton *et al.*, unpublished data.
20. The sequences of the primers are the following: the sense primer, C1, GCAGGCAAGGTATATTTGAAGG [nt 253 through 274 of *CBFB*, (*18*)]; antisense primer 1, or M1, CTCTTCTCCTCATTCTGCTC [reverse sequence of nt 2095 through 2114 of *MYH11*, (*15*)]; antisense primer 2, or M2, ACTGCAGCTCCTGCACCTGC [reverse sequence of nt 1119 through 1138 of *MYH11*, (*15*)].
21. Primers designed to amplify the potential reciprocal fusion transcript were used in RT-PCR with RNA from three inv(16) samples. No PCR products were generated (*9*).
22. N. A. Speck and D. Baltimore, *Mol. Cell. Biol.* **7**, 1101 (1987); J. M. Redondo *et al.*, *ibid.* **12**, 4817 (1992).
23. N. A. Speck *et al.*, *Genes Dev.* **4**, 233 (1990).
24. S. Wang and N. A. Speck, *Mol. Cell. Biol.* **12**, 89 (1992).
25. Y. Kamachi *et al.*, *J. Virol.* **64**, 4808 (1990).
26. E. Ogawa *et al.*, *Virology* **194**, 314 (1993).
27. S. C. Bae *et al.*, *Oncogene* **8**, 809 (1993).
28. E. Ogawa *et al.*, *Proc. Natl. Acad. Sci. U.S.A.*, in press.
29. M. A. Kania, A. S. Bonner, J. B. Duffy, J. P. Gergen, *Genes Dev.* **4**, 1701 (1990).
30. J. D. Rowley, *Ann. Genet.* **16**, 109 (1973).
31. G. Naharro, K. C. Robbins, E. P. Reddy, *Science* **223**, 63 (1984); D. Martin-Zanca, S. H. Hughes, M. Barbacid, *Nature* **319**, 743 (1986).
32. R. Oskam, F. Coulier, M. Ernst, D. Martin-Zanca, M. Barbacid, *Proc. Natl. Acad. Sci. U.S.A.* **85**, 2964 (1988); K. Sugita, J. S. Gutkind, S. Katamine, T. Kawakami, K. C. Robbins, *J. Virol.* **63**, 1715 (1989).
33. D. P. Kiehart, *Cell* **60**, 347 (1990); R. Nagai, D. M. Larson, M. Periasamy, *Proc. Natl. Acad. Sci. U.S.A.* **85**, 1047 (1988).
34. P. Liu, M. B. Perryman, W. Liao, M. J. Siciliano, *Somatic Cell Mol. Genet.* **18**, 7 (1992).
35. Abbreviations for the amino acid residues are as follows: A, Ala; C, Cys; D, Asp; E, Glu; F, Phe; G, Gly; H, His; I, Ile; K, Lys; L, Leu; M, Met; N, Asn; P, Pro; Q, Gln; R, Arg; S, Ser; T, Thr; V, Val; W, Trp; and Y, Tyr.

36. We thank N. Speck for communicating unpublished results and helpful advice and discussions. We thank Y. Ito for allowing us to cite articles in press, M. Drumm for assistance in making the cosmid library, J. Trent for assistance with FISH photography, R. Legerski for the HeLa cDNA library, J. Xu and A. Swaroop for the large intestine cDNA library, K. Yanagisawa for the ME-1 cell line, D. Callen for the chromosome 16 hybrid panel, and R. Stallings for the chromosome 16 cosmid library. P.L. is an associate and F.S.C. was an investigator at the Howard Hughes Medical Institute. Research of D.F.C. and M.J.S. was supported by NIH grant CA55164 and a gift from K. D. Muller (to M.J.S.).

11 May 1993; accepted 2 July 1993

Localization of an Exchangeable GTP Binding Site at the Plus End of Microtubules

T. J. Mitchison

Microtubule polarity arises from the head-to-tail orientation of α-β tubulin heterodimers in the microtubule lattice. The identity of the polypeptide at each end of the microtubule is unknown, but structural models predict that the β-tubulin end contains an exchangeable guanosine triphosphate (GTP) binding site. When GTP-coated fluorescent beads were incubated with microtubules, they bound specifically to plus ends, suggesting that tubulin is oriented in microtubules with β-tubulin toward the plus end.

Microtubules are polar polymers of the protein tubulin. In most cells, the minus ends of microtubules are attached to an organizing center near the cell center, whereas the more peripheral plus ends grow and shrink by dynamic instability (*1*). Tubulin is a heterodimer of α- and β-tubulin subunits, which are 36 to 42% identical in sequence and have similar structures (*2*). The tubulin polypeptides are arranged head-to-tail in the heterodimer and the heterodimers are arranged head-to-tail in the microtubule lattice (*3*), creating a polar lattice. So far it has not been determined which subunit type is exposed at the plus end and which is exposed at the minus end of microtubules.

The polypeptides α- and β-tubulin each bind one molecule of guanine nucleotide with high affinity. The nucleotide binding site on α-tubulin binds GTP nonexchange-

Department of Pharmacology, University of California, San Francisco, CA 94143–0450.

ably and is referred to as the N site. The binding site on β-tubulin exchanges rapidly with free nucleotide in the tubulin heterodimer and is referred to as the E site. On the polymerization of tubulin into microtubules, E site GTP is hydrolyzed to guanosine diphosphate (GDP), which is bound nonexchangeably (*4*). Combining the structural and biochemical data leads to a model in which the β-tubulin end of a microtubule should have an exchangeable GTP binding site (*5*), and this property could be used to infer the orientation of the dimer in the microtubule.

To detect the small number of E sites that might be exposed at one end of a microtubule, we covalently coated 30-nm fluorescent beads with GTP by means of a reaction with the ribose ring (*6*). When a fivefold excess of these GTP-coated beads was incubated with taxol-stabilized microtubules (*7*), many microtubules bound a bead at only one end (Fig. 1A). Adenosine triphosphate (ATP)–coated beads did not associate with microtubules under the same conditions (Fig. 1B). Random fields of microtubules were scored for bead binding under various conditions (Table 1). With GTP-coated beads, 54% of microtubules bound a single bead at one end, and 38% bound no beads. Only 1% bound a bead at both ends. Increasing the concentration of beads 10-fold increased the fraction of microtubules binding beads at a single end to 79%. The fraction binding beads at both ends increased to 3%, probably as a result of increased nonspecific association, as binding to the side also increased. Given the limited resolution of light microscopy, it was not possible to discriminate between beads bound to the end from beads bound on the side near the end. Very little binding at microtubule ends was detected with ATP-coated or nucleotide-free beads. The inclusion of free GTP (1 mM) inhibited end binding to background levels, whereas the inclusion of free ATP (1 mM) caused only a slight reduction in end binding. The binding sites on the ends of microtubules are therefore GTP specific, suggesting that E sites are exposed at one end of the microtubule lattice.

We used three different assays to determine which microtubule end has exposed E sites. (i) Polarity-marked microtubules were made in which the plus end is distinguished by its faster growth rate and appears as the longer, dimly labeled segment emanating from a brightly labeled seed (*8*). GTP beads bound to the plus ends of these microtubules in 95% of the cases scored (Fig. 1, C and D) (*9*). (ii) Polarity-marked microtubules were made in the presence of *N*-ethylmaleimide (NEM)–modified tubulin, which inhibits polymerization from minus ends (*8*). GTP beads bound to the end of the dimly labeled segment (Fig. 1, E and F), again indicating plus-end binding. (iii) GTP beads were added to microtubules elongated from ciliary axonemes (*10*). The faster growth rate of plus ends resulted in a cluster of 5 to 15 long microtubules emanating from the plus end of the axoneme and a cluster of shorter microtubules from the minus end (Fig. 1, G and H). In this

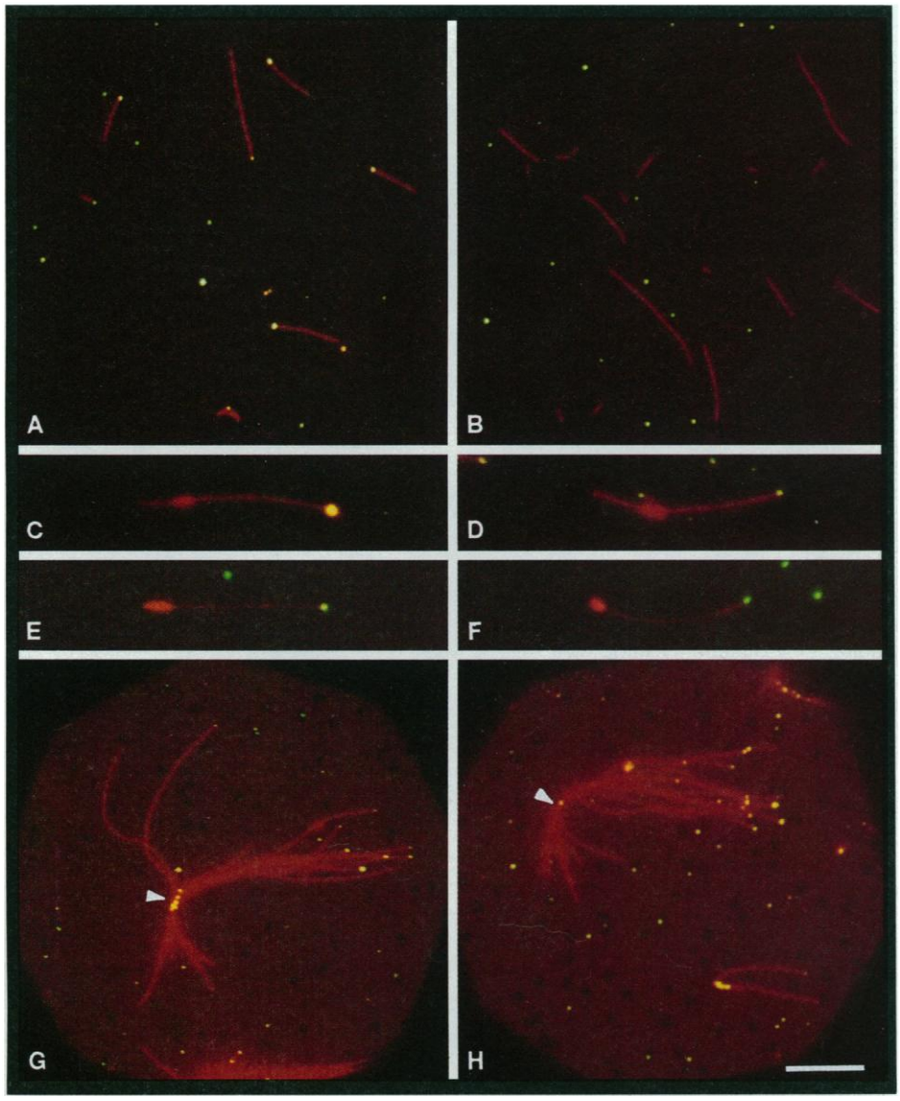

Fig. 1. Binding of nucleotide-coated beads (yellow dots) to taxol-stabilized, tetramethylrhodamine-labeled microtubules (red lines) visualized by fluorescence microscopy. (**A**) Typical field with GTP-coated beads. (**B**) Typical field with ATP-coated beads. (**C** and **D**) Examples of GTP-coated beads bound to polarity-marked microtubules. The plus end of each microtubule is to the right, distinguished by its longer, dimly labeled segment. (**E** and **F**) Examples of GTP-coated beads bound to polarity-marked microtubules prepared in the presence of NEM-tubulin to inhibit minus-end growth. The plus end of each microtubule is to the right, distinguished by its dimly labeled segment. (**G** and **H**) Examples of axonemes elongated with tubulin and incubated with GTP-coated beads. The axoneme is marked with an arrowhead. It tends to bind beads nonspecifically. Microtubules with plus ends distal are pointing rightward and upward, distinguished by their greater length. Note the binding of beads to many plus ends. Microtubules with minus ends distal are pointing downward. No beads are bound to minus ends. Scale bar, 10 μm in (A) and (B); 5 μm in (C) through (F); 15 μm in (G) and (H).

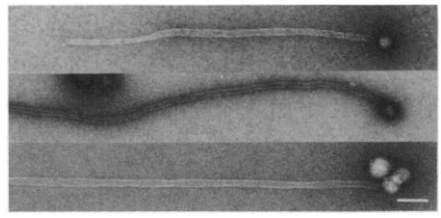

Fig. 2. Microtubules with GTP-coated beads bound to their ends visualized by negative-stain electron microscopy. Scale bar, 100 nm.

Table 1. Statistics of beads bound to microtubules under different conditions. For each condition 200 microtubules were scored in random microscope fields. The numbers show the percentage of microtubules in each category that had a bead bound to one end, beads bound to both ends, beads bound on the side, or no bound beads. The total is more than 100 because a microtubule could have beads bound both to an end and the side. Competing nucleotide was added to 1 mM during incubation with beads. Microtubule number concentration during incubation with beads was approximately 1 nM in all cases. Bead concentration was 5 nM except for the row labeled GTP* in which it was 50 nM.

Nucleotide on beads	Competing nucleotide	Microtubules bound to beads			
		One end (%)	Both ends (%)	Side (%)	None (%)
GTP		54	1	9	38
GTP*		79	3	16	25
ATP		5	0	12	83
None		1	0	4	95
GTP	GTP	2	0	0	98
GTP	ATP	48	0	2	52

assay 97% of the GTP beads scored bound to plus ends (*11*).

To distinguish end binding from near-end binding, we visualized microtubules with GTP-coated beads by negative-stain electron microscopy (*12*). We observed GTP beads bound to the very end of the microtubule (Fig. 2). In some cases small clusters containing two to four beads were observed bound, which explains the variation in fluorescence intensity of beads observed by light microscopy.

To test whether α- or β-tubulin polypeptide binds GTP exchangeably at microtubule ends, we incubated taxol-stabilized microtubules with labeled GTP under conditions in which binding was predominantly to terminal sites, and we cross-linked the GTP to the polypeptide by 260-nm irradiation (*13*). Of the covalently bound GTP, 99% was attached to β-tubulin, and less than 1% was attached to α-tubulin. Thus, the exchangeable GTP-binding sites exposed at the ends of microtubules are on β-tubulin, as was found for soluble tubulin (*14*), and are presumably the same E sites previously identified in the heterodimer.

These results show that exchangeable GTP binding sites on β-tubulin are exposed at the plus ends of microtubules. The simplest interpretation of this result for microtubule structure is that tubulin dimers are oriented in the lattice with β-tubulin toward the plus end, so that the E site on β-tubulin is exposed at that end (Fig. 3). More complex structural models could be considered, but a definitive description of the microtubule lattice will require high-resolution structural analysis.

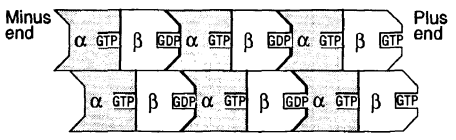

Fig. 3. A simple model for a portion of the microtubule lattice derived from binding of GTP-beads and published structural data (*3, 5*). Nucleotide binding sites on β-tubulin (E sites) in internal lattice positions are nonexchangeable as a result of interactions with neighboring dimers. These sites hydrolyze GTP rapidly. E sites at the plus end of the lattice lack these interactions. They are exchangeable and do not hydrolyze GTP rapidly.

What are the implications of this conclusion? First, knowing the orientation of tubulin in the microtubule lattice will help in understanding how the direction of motor protein movement is controlled (*15*). Second, the structure is relevant to the biology of microtubule ends. Minus ends interact with organizing centers in vivo, perhaps by binding to γ-tubulin. Genetic data suggest that γ-tubulin interacts with β-tubulin (*16*), whereas the GTP-bead data suggest that the terminal polypeptide at the minus end is α-tubulin. If both conclusions are correct, then either γ-tubulin does not bind to the terminal polypeptide, or else the minus end is terminated by a γ-β dimer instead of an α-β dimer. Plus ends undergo dynamic instability in vivo, and their stability may be regulated by a cap of subunits with GTP bound to their E sites (*1*). The GTP-bead data demonstrate the existence of unique, terminal E sites on plus ends which appear not to hydrolyze GTP rapidly (*17*) and may contribute to a GTP cap on the plus end. When microtubules are severed in the presence of tubulin, the new plus ends shrink, whereas the new minus ends resume growth (*18*). This may reflect a requirement for GTP bound to the terminal E sites to stabilize plus ends, whereas minus ends lack this requirement (*5*). Terminal E sites need to be considered in future models for the mechanism of dynamic instability (*19*).

REFERENCES AND NOTES

1. V. I. Gelfand and A. D. Bershadsky, *Annu. Rev. Cell Biol.* **7**, 93 (1991).
2. R. G. Burns, *Cell Motil. Cytoskeleton* **20**, 181 (1991).
3. L. A. Amos and A. Klug, *J. Cell Sci.* **14**, 523 (1974); E. M. Mandelkow and E. Mandelkow, *J. Mol. Biol.* **181**, 123 (1985); L. Beese, G. Stubbs, C. Cohen, *ibid.* **194**, 257 (1987).
4. R. C. Weisenberg, G. G. Borisy, E. W. Taylor, *Biochemistry* **7**, 4466 (1968); M. W. Kirschner, *Int. Rev. Cytol.* **54**, 1 (1978); M. F. Carlier, *ibid.* **115**, 139 (1989).
5. E. Mandelkow and E. M. Mandelkow, in *Cell Movement*, F. D. Warner and J. R. McIntosh, Eds. (Liss, New York, 1989), vol. 2, pp. 23–45.
6. An affinity matrix based on coupling periodate-oxidized GTP to a hydrazide spacer has been described [R. J. Jackson, R. M. Wolcott, T. Shiota, *Biochem. Biophys. Res. Commun.* **2**, 428 (1973)]. We incubated 30-nm, yellow green fluorescent, carboxylate-modified latex microspheres (Molecular Probes L-5201, termed "beads" in this paper) as a 1% suspension with 1 mM bovine serum albumin in 200 mM potassium salt of Pipes (KPipes) and 2 mM EDTA pH 7.0 (PE) at 0°C. Sodium *N*-hydroxysulfosuccinimide was added to 50mM and 1-(3-dimethylamino propyl)-3-ethylcarbodiimide hydrochloride (EDC) was added in portions over 1 hour to 50 mM final concentration. We quenched the reaction by adding lysine to 100 mM and adjusting the pH to 8.5 with Na_2CO_3. The beads were diluted in PE and washed twice by sedimenting them to a total *k*-factor of 50, and the pellet was resuspended in PE. The first resuspension required vigorous sonication to give a uniform suspension. Albumin-coated beads could be stored at 4°C, but it was important to go through the GTP coupling reactions quickly as the intermediates were unstable if stored. Albumin-coated beads were incubated as a 5% suspension in PE containing 20% glycerol at 37°C. Ethylene glycol bis(succinimidyl succinate) was added to 15 mM from a 100 mM stock in DMSO, and the reaction was allowed to proceed for 15 min. The mixture was cooled to 0°C, and hydrazine hydrate added to 200 mM. After 5 min, the reaction was diluted in PE at 0°C and washed twice, as described above. The beads were resuspended after the last wash to give a 5% suspension in 0.2 M sodium salt of MES, 2 mM EDTA, and 50 mM periodate-oxidized GTP (Sigma), pH 6.0, at 0°C. After 5 hours the beads were purified away from excess nucleotide by gel filtration on P10 Biogel equilibrated with 80 mM KPipes, 1 mM $MgCl_2$, and 1 mM EGTA, pH 6.8 (BRB80). The beads were stored in BRB80 containing 50% v/v glycerol at −20°C for up to 1 month without a change in properties. We determined the amount of GTP coupled to the beads by measuring how much γ-phosphate could be transferred to soluble GDP with nucleoside diphosphate kinase (NDPK). Beads were incubated with trace [α-^{32}P]GTP, various levels of cold GDP, and NDPK (10 U/ml) in 50 mM tris-Cl, 5 mM $MgCl_2$, and 7 mM 2-mercaptoethanol, pH 7.5, until equilibrium was reached. Free GTP and GDP were separated by thin-layer chromatography on PEI cellulose in 1.4 M LiCl. GTP-beads had approximately 6000 molecules of GTP bound per bead, corresponding to a surface density of two GTPs per square nanometer.
7. The general methods used are described in A. A. Hyman *et al.* [*Meth. Enzymol.* **196**, 478 (1991)]. Tubulin (40 μM) plus tetramethylrhodamine–labeled tubulin (10 μM) were polymerized in BRB80 containing 1 mM GTP and 10% dimethyl sulfoxide at 37°C for 10 min. We purified the microtubules away from soluble nucleotide by sedimenting them through a cushion containing 60% glycerol and 5 μM taxol in BRB80. The microtubules were resuspended in BRB80 containing 100 μM taxol. In a standard incubation, microtubules at a number concentration of approximately 1 nM (15 μM tubulin polymerized into microtubules of mean length 9 μm) were incubated with 5 nM nucleotide-coated beads in BRB80 containing 30 μM taxol at 25°C for 1 hour with occasional agitation. The microtubules with bound beads were then separated from excess beads by sedimentation through a glycerol cushion as above. The pellet was resuspended in BRB80 plus 30 μM taxol, diluted into BRB80 containing 60% glycerol and 0.1% glutaraldehyde, and mounted for fluores-

cence microscopy. Microtubules with bound beads were observed with a simultaneous fluorescein isothiocyanate and Texas Red filter set (Chroma Technologies) and photographed on Ektachrome P1600 film (Kodak).
8. Polarity-marked microtubules were made as described [A. A. Hyman, *J. Cell Sci. Suppl.* **14**, 125 (1991)]. The marked, taxol-stabilized microtubules were purified away from soluble nucleotide and tubulin and incubated with beads as above.
9. Random microscope fields were selected for scoring. Microtubules that were shorter than the mean length were ignored, because these arise from shearing during pellet resuspension, as were microtubules that showed evidence of annealing (multiple bright segments). Of 200 microtubules scored, 190 had a bead bound only to the plus end, 6 only to the minus, and 4 to both ends.
10. L. G. Bergen, R. Kuriyama, G. G. Borisy, *J. Cell Biol.* **84**, 151 (1980). Tetrahymena axonemes were diluted in BRB80 and adsorbed to cover slips in perfusion chambers, which were then blocked with casein (10 mg/ml). Tubulin (24 μM) plus tetramethylrhodamine-labeled tubulin (6 μM) in BRB80 containing 1 mM GTP, 7 mM 2-mercaptoethanol, and 2% polyethylene glycol 8000 was perfused in and allowed to polymerize for 6 min at 37°C. The chambers were washed extensively with BRB80 containing 30 μM taxol; then 5 nM GTP-coated beads in the same buffer were perfused in and incubated for 1 hour. The chambers were washed and viewed by fluorescence microscopy. Initially the microtubules were not adherent to the substrate, and beads attached to plus ends were observed moving around attached to microtubule plus ends. For photography, we stuck down the microtubules by perfusing 100 nM kinesin into the chambers, followed by BRB80 containing 60% glycerol and 0.1% glutaraldehyde.
11. We scored 38 axonemes after photography. We observed 209 beads associated with plus ends and 6 with minus ends. The background sticking of beads to the cover slip near a microtubule end probably accounts for the minus-end binding.
12. Microtubule preparation and incubation with beads was as in (*7*) except that tetramethylrhodamine-labeled tubulin was omitted. The final microtubule pellet was diluted in BRB80 containing 30 μM taxol, adsorbed to freshly glow-discharged Formvar- and carbon-coated grids, negatively stained with 1% uranyl acetate, and imaged at 80 kV.
13. Taxol-stabilized microtubules were prepared free of soluble tubulin and GTP as in (*7*), and an aliquot was removed for determining number concentration by quantitative sedimentation onto cover slips. We incubated [α-^{32}P]GTP at various specific activities with microtubules in BRB80 containing 30 μM taxol for 3 min and then sedimented the microtubules through a glycerol-containing cushion to remove unbound nucleotide. The amount of bound nucleotide was determined by scintillation counting of the pellet, and the specific activity was corrected for the small amount of nucleotide present in the washed microtubule preparation and the low level of nonspecific binding. Under these conditions, the nucleotide was bound primarily to terminal E sites by two criteria: (i) Bound to each microtubule end were 10 ± 3 molecules of GTP. (ii) Up to 70% of the bound nucleotide in samples not subject to cross-linking was recovered as unhydrolyzed GTP. Nucleotide recovered from internal E sites was 100% hydrolyzed to GDP in control experiments. We cross-linked [α-^{32}P]GTP to tubulin by exposing the microtubule pellets to 260-nm light, as described for soluble tubulin (*13*). The α- and β-tubulin were resolved by electrophoresis in polyacrylamide gels containing sodium dodecyl sulfate contaminated with higher molecular weight alkyl chains. We confirmed the identity of the subunits (β-tubulin runs faster) by immunoblotting with monoclonal antibodies. Bands corresponding to α- and β-tubulin were excized and counted. Of the counts 99% were in the β-tubulin band and less than 1% in the α-tubulin band.
14. J. P. Nath, G. R. Eagle, R. H. Himes, *Biochemistry* **24**, 1555 (1985).
15. R. B. Vallee and H. S. Shpetner, *Annu. Rev. Biochem.* **59**, 909 (1990).
16. B. R. Oakley, *Trends Cell Biol.* **2**, 1 (1992).
17. Chemically cross-linked and sheared microtubules were reported to lack intrinsic GTPase activity [M. Caplow and J. Shanks, *J. Biol. Chem.* **265**, 8935 (1990)]. In preliminary experiments, we observed that [α-^{32}P]GTP bound to terminal E sites of taxol-stabilized microtubules (*13*) underwent much slower hydrolysis than nucleotide bound to internal E sites.
18. R. A. Walker, S. Inoue, E. D. Salmon, *J. Cell Biol.* **108**, 931 (1989).
19. I thank A. Hyman, M.-L. Wong, F. Malik, and P. Siebert for technical and intellectual help and K. Sawin and J. Howard for comments. This work was funded by NIH grant GM-39565 and a fellowship from the Packard Foundation.

22 March 1993; accepted 14 June 1993

Amyotrophic Lateral Sclerosis and Structural Defects in Cu,Zn Superoxide Dismutase

Han-Xiang Deng, Afif Hentati, John A. Tainer, Zafar Iqbal, Annarueber Cayabyab, Wu-Yen Hung, Elizabeth D. Getzoff, Ping Hu, Brian Herzfeldt, Raymond P. Roos, Carolyn Warner, Gang Deng, Edwin Soriano, Celestine Smyth, Hans E. Parge, Aftab Ahmed, Allen D. Roses, Robert A. Hallewell, Margaret A. Pericak-Vance, Teepu Siddique*

Single-site mutants in the Cu,Zn superoxide dismutase (SOD) gene (*SOD1*) occur in patients with the fatal neurodegenerative disorder familial amyotrophic lateral sclerosis (FALS). Complete screening of the *SOD1* coding region revealed that the mutation Ala^4 to Val in exon 1 was the most frequent one; mutations were identified in exons 2, 4, and 5 but not in the active site region formed by exon 3. The 2.4 Å crystal structure of human SOD, along with two other SOD structures, established that all 12 observed FALS mutant sites alter conserved interactions critical to the β-barrel fold and dimer contact, rather than catalysis. Red cells from heterozygotes had less than 50 percent normal SOD activity, consistent with a structurally defective SOD dimer. Thus, defective SOD is linked to motor neuron death and carries implications for understanding and possible treatment of FALS.

Amyotrophic lateral sclerosis (ALS), also called motor neuron disease, Charcot's disease, or Lou Gehrig's disease, is a progressive paralytic disorder that is usually fatal within 5 years of onset of symptoms (*1*). The paralysis is due to degeneration of large motor neurons of the brain and spinal cord; the underlying cause of the degeneration is not known (*2*). About 10% of ALS cases are familial. Familial ALS (FALS), clinically indistinguishable from sporadic ALS, is expressed as an age-dependent autosomal dominant trait (*3*, *4*). *SOD1*, the gene encoding the cytosolic antioxidant enzyme Cu,Zn superoxide dismutase (SOD), was studied as a FALS candidate because of (i) its proximity to a FALS locus mapped to chromosome 21q22.1 in a subset of FALS families (*5*–*7*), (ii) decreased SOD activity in cerebrospinal fluid of some ALS patients (*8*), (iii) the important function of SOD in free radical homeostasis (*9*), and (iv) the apparent role of free radicals in neurodegeneration (*10*). For 7 of the 11 previously reported FALS families (*5*, *6*) the probability of genetic linkage, based on heterogeneity analysis (*11*), to the region containing *SOD1* on chromosome 21 (*7*) was >90% (*6*). For three of the remaining families, linkage to this region was excluded; and for the fourth, results were inconclusive (*6*). Mutations in *SOD1* have been described in FALS families (*12*) but examined in only two (exons 2 and 4) of the five *SOD1* exons. The effects of the mutations on the enzyme's structure and function were not identified: they were hypothesized either to reduce or to increase the SOD activity. We now present the combined results from

H.-X. Deng, A. Hentati, A. Cayabyab, W.-Y. Hung, P. Hu, B. Herzfeldt, G. Deng, E. Soriano, C. Smyth, A. Ahmed, Department of Neurology, Northwestern University Medical School, 300 E. Superior Street, Chicago, IL 60611.
J. A. Tainer, E. D. Getzoff, H. E. Parge, Department of Molecular Biology, The Scripps Research Institute, La Jolla, CA 92037.
Z. Iqbal, Department of Neurology, Northwestern University Medical School, Chicago, and Northwestern University Institute of Neuroscience, Chicago, IL 60611.
R. P. Roos, Department of Neurology, University of Chicago, Chicago, IL 60637.
C. Warner, Department of Neurology, Dent Neurological Institute, Buffalo, NY 14209.
A. D. Roses and M. A. Pericak-Vance, Department of Medicine (Neurology), Duke University Medical Center, Durham, NC 27710.
R. A. Hallewell, Department of Biochemistry, Imperial College, London SW7 2AZ, U.K.
T. Siddique, Departments of Neurology and of Cell, Molecular, and Structural Biology, Northwestern University Medical School, Chicago, IL 60611, and Northwestern University Institute of Neuroscience.

*To whom requests for reprints should be addressed.